Research Article | Vol. 28, No. 10 / 11 May 2020 / Optics Express 15250

Optics EXPRESS

Check for updates

Measurement of slow and fast polarization transients on a fiber-optic testbed

PETER BARCIK* AND PETR MUNSTER

Brno University of Technology, Technicka 12, 616 00 Brno, Czech Republic
*barcik@feec.vutbr.cz

Abstract: Polarization changes inside a single-mode fiber due to birefringence are studied in this paper. We demonstrate a measurement system for the detection of fast and slow polarization transients in a single-mode optical fiber route. The output signals from a polarimeter based on tilted fiber gratings and a polarimeter based on a polarizing beam splitter and a balanced detector (PBS polarimeter) are processed. The processed data reveal that the detected signal depends on the vibration along the fiber route caused by trains and the temperature instability around the fiber. The proposed system is sufficient for detecting polarization transients and can be used for the detection of suspicious events that would lead to a disruption of the optical path.

Published by The Optical Society under the terms of the Creative Commons Attribution 4.0 License. Further distribution of this work must maintain attribution to the author(s) and the published article's title, journal citation, and DOI.

1. Introduction

The propagation of optical waves in various media is still of interest, because continuously improving technologies are adopted in sensing and communication systems. Polarization is one of the properties of an optical wave that has been studied very intensively. Accurate knowledge of the polarization allows one to measure more precisely or communicate faster, safer, and more effectively. In optical fiber communication technology, polarization impairments can be problematic for high-speed (10G) transmissions. The mechanical and optical properties of an optical fiber change due to applied mechanical stress, acoustic vibrations and temperature changes. These disturbances change the local refractive index of the fiber core and give rise to birefringence. Birefringence results in different propagation speeds of the optical wave along the x and y axes of the fiber, which leads to polarization mode dispersion (PMD). In contrast to chromatic dispersion (CD), PMD is not stable in time. This makes it hard to compensate PMD passively, and more sophisticated compensation systems have to be deployed [1].

There are a number of papers that have addressed compensation and monitoring of polarization transients in optical fiber routes [2]. The characterization of polarization transients is critical for designing digital coherent receivers that must handle the transients [3]. Long-term observation of the state of polarization (SOP) in an installed fiber route was introduced in [4]. The paper presented field observations over 18 months. Monitoring techniques for high-capacity optical networks were studied in [5]. The authors addressed monitoring of the optical signal-to-noise ratio (OSNR), CD and PMD for different modulation formats.

Because SOP variations are dependent on disturbances applied to the fiber, one can advantageously use these variations for sensing. A long fiber optic route was used for pipeline leakage, intrusion and ground movement detection in [6]. In [7], SOP transients inside optical fiber buried in the ground were employed to detect lightning strikes. The sensing ability of the optical fiber can also be used to improve the safety and reliability of the connection. The concept of proactive fiber damage detection in the monitoring channel was introduced in [8] and [9].

To measure the polarization properties of an optical wave, one can use a polarimeter. The polarimeter has to be fast enough to observe very fast polarization transients. In optical fiber technology, fast inline polarimeters are usually used [10]. The fast inline polarimeters are based

#390649 https://doi.org/10.1364/OE.390649
Journal © 2020 Received 17 Feb 2020; revised 3 Apr 2020; accepted 3 Apr 2020; published 5 May 2020

on detection of a polarization-dependent scattered light from tilted fiber gratings. The scattered light is detected by four separated photodiodes. More affordable polarimeters are based on a polarizing beam splitter [11].

The main motivation of this paper is to present a system for polarization analysis of the optical wave in an optical fiber. The theoretical background and methodology are described in Chapter 2. In Chapter 3, the proposed system is deployed for a real fiber route to verify its functionality. Then, the polarization properties of the optical wave inside the fiber are investigated. In this paper, we focus on monitoring fast and slow polarization transients. Chapter 4 describes two measurement campaigns. The first campaign focuses on the detection of fast transients caused mainly by trains that pass along the fiber route. The second campaign focuses on slow transients caused mainly by temperature changes.

The novelty of this paper is the comparison of a simple polarization detection technique based on a polarizing beam splitter with a more sophisticated method based on a fast fiber polarimeter. From the experimental measurement campaigns deployed for the real fiber route, valuable experimental data are gathered.

2. Theoretical background and methodology

It is generally known that the refractive index in isotropic optical materials is the same in each polarization direction. In the case of anisotropic materials, the refractive index is different in different polarization directions. This also applies to optical fibers. If an optical fiber is symmetrical in all length directions, no birefringence will be present. The optical wave will spread ideally in two orthogonal planes. The refractive index in one polarization plane would be the same as the refractive index in the second plane $n_x = n_y$, and the propagation parameters would be the same for both polarization planes $\beta_x = \beta_y$. In real optical fibers, the situation is slightly more complicated. Optical fiber is a transmission medium with birefringence. The constants for the spreading of optical signals are different for both polarization planes $\beta_x \neq \beta_y$. If the birefringence is characterized by $\triangle\beta$, we can express this parameter as [12]:

$$\triangle\beta = \beta_y - \beta_x = \frac{2}{\lambda}\left(n_y - n_x\right) = \frac{\omega}{c}\Delta n, \tag{1}$$

where ω is the angular frequency, n is the refractive index and c is the speed of the light. The birefringence in optical fibers causes changes in the SOP.

The difference in the propagation constants for two orthogonal axes leads to a change in the phase difference between the two fundamental modes inside the fiber with length L [13]

$$\triangle\phi = \triangle\beta L, \tag{2}$$

where $\beta = kn$, $k = 2\pi/\lambda$ is the optical wavenumber and L is the length of the fiber.

The phase difference generated by longitudinal strain and temperature changes can be described by the following relations [13]:

$$\frac{\delta\left(\triangle\phi\right)}{\delta\epsilon} = \triangle\beta\frac{\delta\left(\triangle L\right)}{\delta\epsilon} + L\frac{\delta\left(\triangle\beta\right)}{\delta\epsilon}, \tag{3}$$

$$\frac{\delta\left(\triangle\phi\right)}{\delta T} = \triangle\beta\frac{\delta\left(\triangle L\right)}{\delta T} + L\frac{\delta\left(\triangle\beta\right)}{\delta T}, \tag{4}$$

where ϵ is the strain and T is the temperature.

3. Field measurement of the polarization transients

Figure 1(a) shows the setup that is used for our field experiment. The experimental setup for measuring the polarization transients was installed at the train station in the city Tisnov in

Optics EXPRESS

the Czech Republic. As a light source, we used a low-noise distributed-feedback (DFB) laser (Koheron LD101) with a wavelength of 1550 nm and a spectral linewidth of 3 MHz. According to laser manufacturer, the Relative Intensity Noise (RIN) at the signal frequency 10 Hz and operating current 50 mA is -115 dBc/Hz and at the signal frequency 1 MHz it is -156 dBc/Hz. The output optical power of the laser is 4.8 dBm, and the laser has an integrated optical isolator. Continuous-wave light was input into a single-mode (SM) fiber route used for the measurement (testbed), which is buried along the railroad between the cities Vlkov and Tisnov in the Czech Republic (see Fig. 1(b)). In Vlkov, the fiber is looped back to Tisnov. The length of the whole fiber testbed is approximately 40 km. The other side of the SM fiber is connected to polarimeters. Half of the received optical power is connected to the fast polarimeter (block A), and half of the power is connected to the PBS polarimeter (block B).

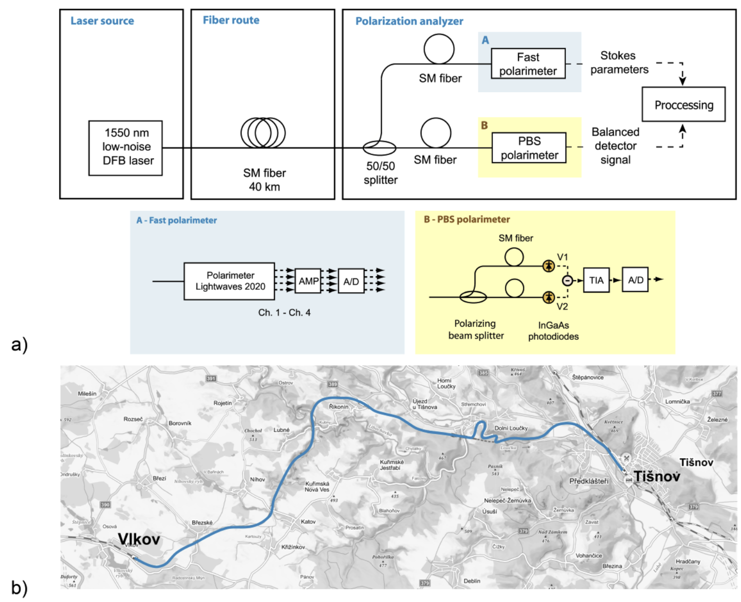

Fig. 1. a) Experimental setup for measuring the polarization transients. b) Map of the testbed from Tisnov to Vlkov in the Czech Republic.

Block A (see Fig. 1(a)) consists of the polarimeter Lightwave 2020 model PRIME0000000514. The polarimeter works based on the principle of light scattering on the tilted gratings in the optical fiber. Polarization-sensitive scattered light is detected by four photodiodes (Ch. 1 - Ch. 4). The output currents are amplified and converted to four voltages. To process the received voltages, we used the development platform National Instruments Rio to record and save the data. Every channel is sampled at a sampling frequency of 25 kHz. The polarimeter was calibrated by a Thorlabs IPM5300-T precision polarimeter. After the calibration of the polarimeter, the four voltages were transformed into the Stokes parameters. To quantify the polarization transients in the SM optical fiber, the polarization rotation rate (PRR) was used. The PRR determines the speed of the central angle change between two points that lie on the Poincaré sphere. Because these points are determined by the Stokes parameters, it is possible to calculate the PRR as follows [9]:

$$\Delta\sigma_{Pol} = 2\sin^{-1}\left(\frac{\sqrt{(\Delta S_1)^2 + (\Delta S_2)^2 + (\Delta S_3)^2}}{2}\right)\frac{1}{\Delta t_p}, \tag{5}$$

where Δt_p is the sampling period of the fast polarimeter.

Optics EXPRESS

Block B (see Fig. 1(a)) consists of a polarizing beam splitter that splits the optical wave into two optical waves with orthogonal polarizations. The optical waves are detected by an InGaAs amplified balanced detector with a bandwidth of 100 MHz. Because a transimpedance amplifier (TIA) is used in the detector, the optical receiver has better sensitivity than the optical receivers in the fast polarimeter. The output signal from the balanced detector (V_1 and V_2) is digitized by the acquisition platform Red Pitaya. The maximal sampling frequency is 125 MHz. The PRR from the balanced detector signal is calculated as [9]:

$$\Delta\sigma_{Bal} = 2\sin^{-1}\left(\frac{1}{2}\Delta\left[\left|\frac{V_1 - V_2}{V_1 + V_2}\right|\right]\right)\frac{1}{\Delta t_b}, \tag{6}$$

where Δt_b is the sampling period of the polarimeter based on PBS.

The sensitivity of the PBS polarimeter depends on the state of the polarization before the polarizing beam splitter. To illustrate the sensitivity we calculated the relative balanced detector sensitivity ξ as a function of polarization state specified before polarizing beam splitter. After simplification the relative sensitivity can be calculated as follows

$$\xi = \frac{1}{2}\left(\sin(2\chi)^2 + \sin(2\psi - 2\chi)^2\right), \tag{7}$$

where ψ and χ are orientation and ellipticity angles of polarization ellipse. In Fig. 2 the sensitivity of the balanced detector is depicted on Poincaré sphere. The system is maximally sensitive when the polarization of the optical wave is rotated to an angle $\pi/4$ with respect to the polarizing beam splitter axes. On the other hand, when the polarization of the optical wave is parallel to the x and y axes of the polarizing beam splitter, the sensitivity is minimal.

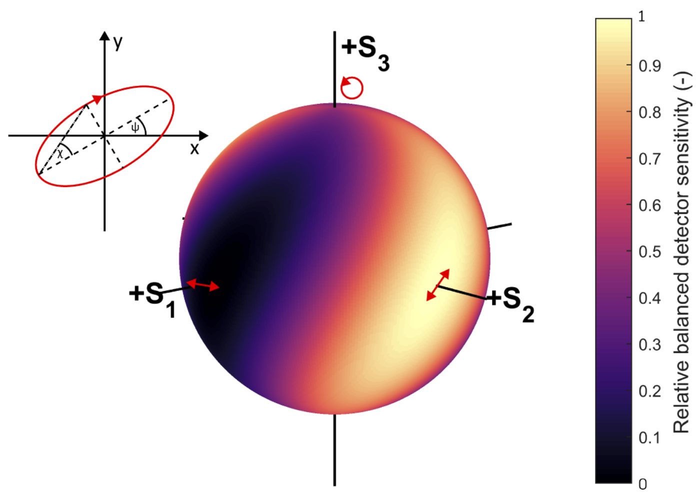

Fig. 2. Theoretically calculated relative balanced detector sensitivity as a function of polarization state before polarizing beam splitter depicted on Poincaré sphere.

4. Results and discussion

In the first experiment, we measured the fast elastic polarization transients caused by external disturbances along the optical fiber route. Because the fiber route is buried along the train track, the polarization transients are caused mainly by vibrations from the carriages of the train. Because the analysis system measures only the PRR integrated along the whole fiber route, it is not possible to spatially detect the source of the disturbance event within the fiber route. However,

Optics EXPRESS

we found from the measured data that certain places along the fiber route are more sensitive than others. In Fig. 3(a) and Fig. 3(b), we depict a 20-minute-long signal of the PRR to compare both detection systems. It is clear that there are two significant events between the fourth and sixth minutes and between the fourteenth and sixteenth minutes, which are detected sufficiently by both systems. These events correspond to places where the train passes the bridge. The reason for this sensitivity is that the fiber is not buried and it is placed in a cable tray on the bridge. By measuring the time difference between these two significant peaks (if the length of the bridge is known), one can approximately calculate the speed of the train on the bridge. The difference between the amplitudes of the detected PRR is mainly due to the different gains and different sampling frequencies of the optical receivers in the PBS polarimeter and fast polarimeter. The information about the polarization state of the received optical wave from the PBS polarimeter was processed with a fast Fourier transform (FFT) algorithm and depicted by a spectrogram (see Fig. 3(c)). It is easier to detect polarization transient events with the spectrogram than with the time signal.

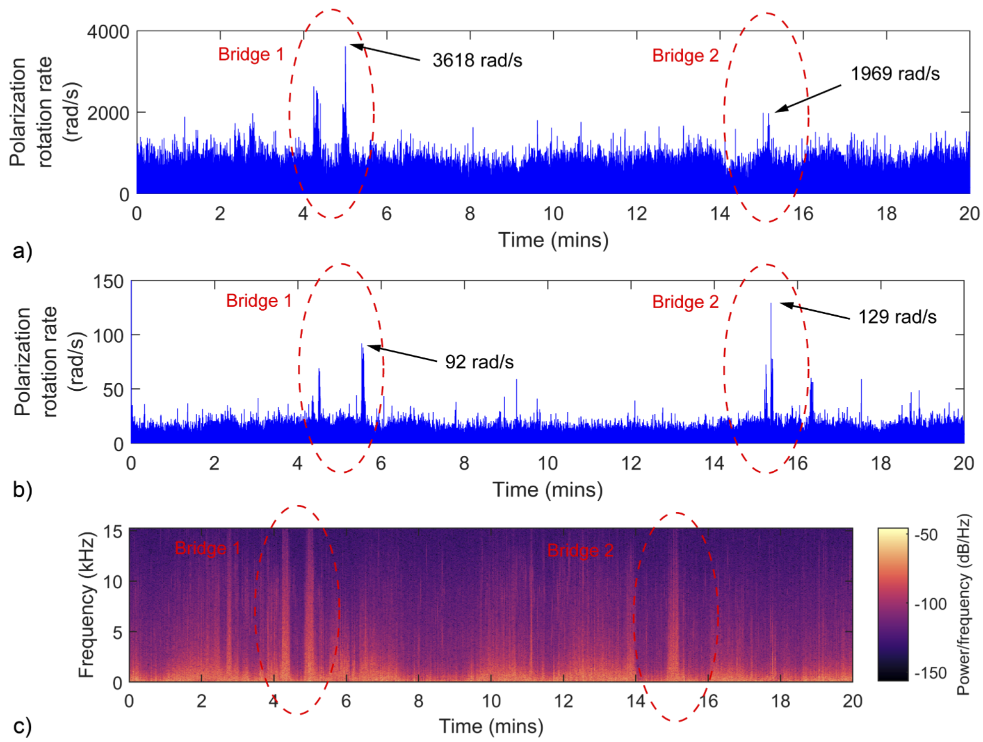

Fig. 3. The measured data from the measurement campaign carried out on the testbed (November 25, 2019, starting at 11:05 and ending at 11:25): the a) PRR measured by the PBS polarimeter, b) PRR measured by the fast polarimeter, and c) spectrogram of the signal recorded by the balanced detector.

In the second experiment, we logged the polarization rotation rate during a three-day measurement campaign. Figure 4(a) depicts the PRR measured by the balanced detector. To determine the slow inelastic polarization transients, the sampling rate was decreased to 30 Hz. Additionally, during the postprocessing, the data were smoothed by a moving average (MA) filter over period of 0.5 hour and 5 hour. As shown in Fig. 4(a), there is an obvious clear diurnal dependence of the PRR on the temperature changes. The PRR is minimal during the night and maximal during the day. The visible peaks, which are modulated on the slow signal, correspond to the train passing the track. The diurnal dependence is also evident from the measurement performed by the fast polarimeter (see Fig. 4(b)). To analyze the similarity between the PRR and temperature, we depict the temperature (Fig. 4(c)) measured by a meteorological station located near the city Brno. For a better comparison, the temperature data were detrended.

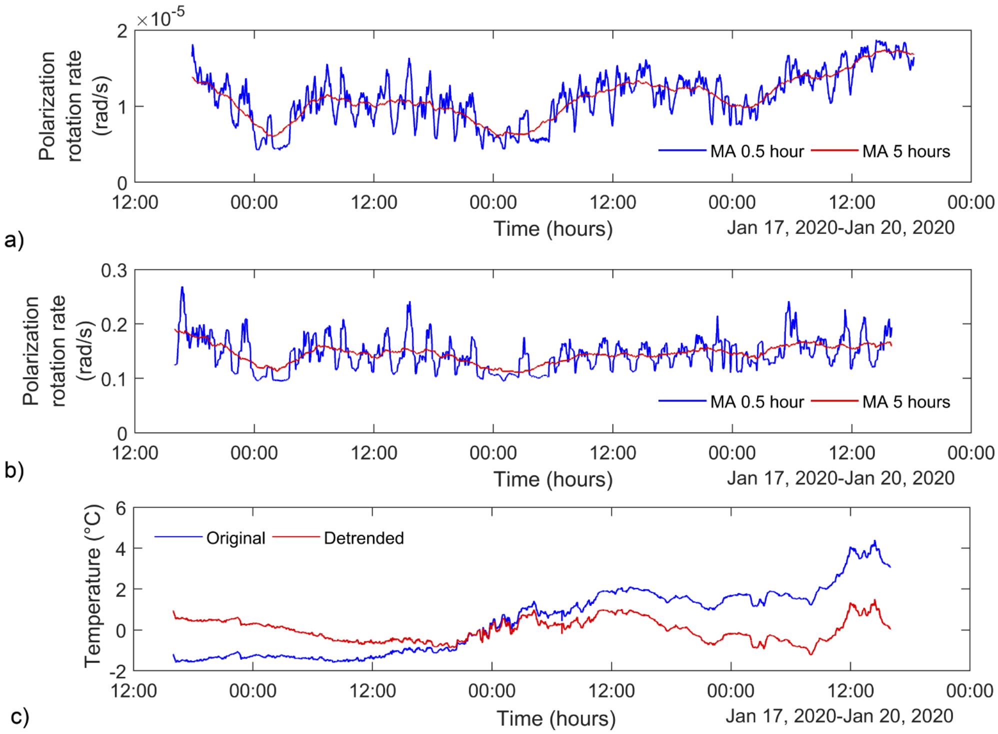

Fig. 4. The measured data from the measurement campaign carried out on the testbed (January 17 - 20, 2020, starting at 16:00 and ending at 16:00): a) PRR measured by the PBS polarimeter, b) PRR measured by the fast polarimeter, and c) measured air temperature.

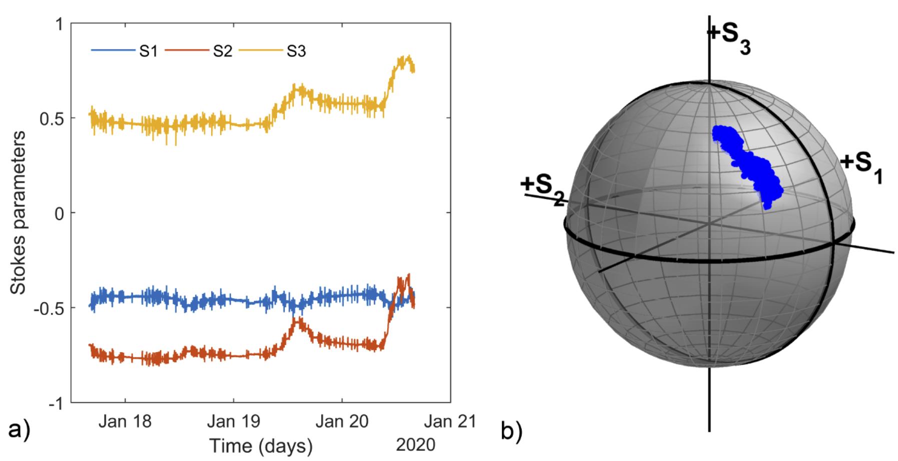

Fig. 5. a) Stokes parameters measured by the fast polarimeter. b) Stokes parameters represented by the Poincare sphere.

Figure 5(a) shows the normalized Stokes parameters recorded by the fast polarimeter. These data reveal a clear relationship between slow temperature changes (Fig. 4(c)) and a change in the Stokes parameters. The fast transients caused by trains are also visible in the Stokes parameter data. In Fig. 5(b), all of the data are plotted on the Poincaré sphere.

The output signal from the PBS polarimeter does not provide complete information about the polarization state of the optical wave. The system does not measure the ellipticity of the polarization. Nonetheless, the proposed system achieves sufficient results in comparison with a standard polarimeter. Employing the presented system, one can easily detect activity around the fiber route. The detection of unwanted activity can be used to increase the reliability of the optical fiber link. The future work will be focused on monitoring of the polarization transients in the optical fiber link with data traffic together with design of a new PBS polarimeter which eliminates dependency of the sensitivity on polarization state of the optical wave.

5. Conclusion

We experimentally tested the ability of a PBS polarimeter to detect fast and slow polarization transients in a fiber route. We performed two measurement campaigns. The analysis of the data showed that we can detect a train passing along the fiber route. The temperature dependence of the detected signal was also presented. To assess the performance of the system, the polarization was simultaneously recorded by a fast polarimeter.

Funding

Ministerstvo Vnitra České Republiky (VI20152020045).

Acknowledgments

The work has been supported by EUIMWP (CA 16220) COST Action. Acknowledgment is also given to CESNET for technical support and the equipment used for the experiments. Portions of this work were presented at the Asia-Pacific Optical Sensors Conference (APOS) in 2019, "Measurement of Polarization Transient Effects in Data Signal due to Mechanical Stress Applied to Optical Fibre".

Disclosures

The authors declare no conflict of interest.

References

1. D. Derickson, *Fiber Optic Test and Measurement* (Prentice-Hall, Inc., 1998).
2. M. Brodsky, N. J. Frigo, M. Boroditsky, S. Member, and M. Tur, "Polarization Mode Dispersion of Installed Fibers," J. Lightwave Technol. **24**(12), 4584–4599 (2006).
3. L. E. Nelson, M. Birk, S. L. Woodward, and P. Magill, "Field measurements of polarization transients on a long-haul terrestrial link," IEEE Photonic Soc. 24th Annu. Meet. PHO 2011 **5**, 833–834 (2011).
4. S. L. Woodward, S. Member, L. E. Nelson, S. Member, C. R. Schneider, L. A. Knox, M. O. Sullivan, C. Laperle, M. Moyer, and S. Foo, "Long-Term Observation of PMD and SOP on Installed Fiber Routes," IEEE Photonics Technol. Lett. **26**(3), 213–216 (2014).
5. C. Lu, L. P. T. Lau, F. N. Khan, Q. Sui, J. Zhao, Z. Li, H. Y. Tam, and P. K. Wai, "Optical performance monitoring techniques for high capacity optical networks," in *2010 7th International Symposium on Communication Systems, Networks and Digital Signal Processing, CSNDSP 2010* pp. 678–681 (2010).
6. M. Nikles, "Long-distance fiber optic sensing solutions for pipeline leakage, intrusion, and ground movement detection," Proc. SPIE **7316**, 731602 (2009).
7. D. Charlton, S. Clarke, D. Doucet, M. O'Sullivan, D. L. Peterson, D. Wilson, G. Wellbrock, and M. Bélanger, "Field measurements of SOP transients in OPGW, with time and location correlation to lightning strikes," Opt. Express **25**(9), 9689 (2017).
8. F. Boitier, V. Lemaire, J. Pesic, L. Chavarría, P. Layec, S. Bigo, E. Dutisseuil, N. B. Labs, and R. D. Villejust, "Proactive Fiber Damage Detection in Real-time Coherent Receiver," in *2017 European Conference on Optical Communication (ECOC)*, (2017), 1, pp. 2–4.

Optics EXPRESS

9. P. J. Simsarian and J. E. Winzer, "Shake before break: Per-span fiber sensing with in-line polarization monitoring," in *Optical Fiber Communications Conference and Exhibition (OFC)*, (2017), pp. 1–3.
10. V. Mikhailov, B. A. Rabin, and P. S. Westbrook, "In-line high-speed all-fiber polarimeter with true real-time acquisition for sensor systems based on fast polarization rotation," J. Lightwave Technol. **33**(12), 2679–2684 (2015).
11. V. Lecœuche, F. Sauron, A. Champavère, and F. Heismann, "Non-Intrusive PMD Measurements on Active Fiber Links Using a Novel Coherent Polarization Analyzer," Tech. rep., JDSU (2012).
12. H. E. Francis and A. Jenkins, *Fundamentals of Optics* (The McGraw-Hill Companies, Inc., 2001), 4th ed.
13. T. R. Woliński, P. Lesiak, and A. W. Doma nski, "Polarimetric optical fiber sensors of a new generation for industrial applications," Bull. Pol. Acad. Sci.: Tech. Sci. **56**(2), 125–132 (2008).

147.229.117.44 {ts '2020-05-29 02:37:40'}